Magnetic Trapping and Zeeman Relaxation of NH ($X\,^3\Sigma^-$)

Wesley C. Campbell,[1,2,*] Edem Tsikata,[1,2] Hsin-I Lu,[3,2] Laurens D. van Buuren,[1,2,†] and John M. Doyle[2,1]

[1]*Department of Physics, Harvard University, Cambridge, Massachusetts 02138, USA*
[2]*Harvard-MIT Center for Ultracold Atoms, Cambridge, Massachusetts 02138, USA*
[3]*Division of Engineering and Applied Sciences, Harvard University, Cambridge, Massachusetts 02138, USA*

(Received 5 February 2007; published 25 May 2007)

NH radicals are magnetically trapped and their Zeeman relaxation and energy transport collision cross sections with helium are measured. Continuous buffer-gas loading of the trap is direct from a room-temperature molecular beam. The Zeeman relaxation (inelastic) cross section of magnetically trapped electronic, vibrational, and rotational ground state NH molecules in collisions with ^{3}He is measured to be $3.8 \pm 1.1 \times 10^{-19}$ cm^2 at 710 mK. The NH-He energy transport cross section is also measured, indicating a ratio of diffusive to inelastic cross sections of $\gamma = 7 \times 10^4$, in agreement with recent theory [R. V. Krems, H. R. Sadeghpour, A. Dalgarno, D. Zgid, J. Kłos, and G. Chałasiński, Phys. Rev. A **68**, 051401 (2003)].

DOI: 10.1103/PhysRevLett.98.213001 PACS numbers: 33.80.Ps, 39.10.+j

Driven by the promise of new physics and applications, the field of cold molecular physics has undergone tremendous growth in the past decade [1,2]. In particular, polar molecules have been proposed as qubits for quantum information processing [3,4] and for studies of highly correlated condensed matter systems [5]. Cold molecules are also very promising candidates for fundamental physics measurements, such as the search for the electric dipole moment of the electron [6] and time variation of the electron-proton mass ratio [7]. Chemistry with cold molecules may be possible to observe in a new quantum regime where the large de Broglie wavelength and long interaction times of reactants can reopen chemical reaction pathways through tunneling [8,9]. A key to realizing these new phenomena is the production of cold, trapped, high-density samples of polar molecules.

The complexity inherent in molecules, compared to atoms, makes working with them difficult; the rich internal structure of molecules opens decay modes that, for example, could make evaporative cooling difficult to achieve [10]. Preparation of cold, dense samples of trapped molecules should provide a pathway to measure cold molecule collisions, critical to elucidating the suitability of molecules for evaporative [11–13] and sympathetic cooling [14]. So far, several methods have been used to create (ultra-)cold molecules. Production of ultracold molecules from ultracold atoms has been realized through photo and Feshbach association [15,16]. Direct cooling or slowing of initially hot polar molecules has also been demonstrated using Stark deceleration [2,17], optical slowing [18], billiardlike collisions [19], and buffer-gas cooling [20]. Buffer-gas cooling uses cryogenic helium gas to cool hot molecules (or atoms). When done in the presence of a magnetic trapping field this can cause the molecules to fall into the conservative trap potential. The first successful trapping of polar molecules was accomplished in our group with buffer-gas loading of CaH, and we know of several other laboratories using buffer-gas loading of magnetic traps [21–23]. Other molecules (VO [24], CaF [25], and CrH [26]) have also been studied with buffer-gas loading.

Despite great progress in the field of cold molecules, no technique has yet realized trapped densities sufficiently high to observe polar molecule-molecule collisions. However, the buffer-gas method allowed studies of cold atom-polar molecule spin relaxation of trapped molecules (He-CaH and CaF [20,25]). Collisional quenching of rotational and electronic excited states has been seen in earlier experiments [27–29]. The buffer-gas cooling measurements in Ref. [20,25] in combination with theory, began to uncover the fundamental processes of cold molecule spin-relaxation collisions in traps. CaH has a $^2\Sigma$ ground state, perhaps the simplest type of magnetically trappable molecule. $^3\Sigma$ molecules, however, carry with them new internal dynamics, such as the spin-spin interaction, which allows for direct coupling of the rotation during a collision (unlike the $^2\Sigma$ case) [30]. The current vigorous pursuit of high-density samples of cold molecules has led several groups to the NH radical. Cold, trapped NH is being studied theoretically [13,14,31,32] and pursued experimentally [33–35], and a scheme for continuous loading of NH into a magnetic trap has been proposed for Stark deceleration [36].

In this Letter, we demonstrate magnetic trapping of ground state ($X\,^3\Sigma^-$) NH radicals and make a direct measurement of the spin-relaxation rate in collisions with ^{3}He. NH is continuously loaded directly from a room-temperature molecular beam into a magnetic trap *via* buffer-gas cooling. More than 10^8 molecules are loaded into the trap and are observed for longer than 1 s, with $1/e$ lifetimes exceeding 200 ms. The maximum trap depth achieved exceeds the buffer-gas temperature by a factor of $\eta = 6.5$. The energy transport collision rate with ^{3}He is also measured, allowing the determination of the ratio of the diffusive to inelastic cross sections in this system, found to be $\gamma = \sigma_d/\sigma_{\text{in}} = 7 \times 10^4$.

Our motivations for choosing the NH radical are described elsewhere [34]. The production of NH radicals in a

high-flux beam with a room-temperature discharge source provides a new experimental challenge—the introduction of this beam into our very low temperature region. This was a key experimental challenge that was met with success and can be applied to numerous other species.

Our apparatus is centered around a copper cold cell [37] that is thermally disconnected from the 4 K magnet surrounding it (see Fig. 1). The maximum trap depth available is 3.9 T. Windows at the magnet midplane allow optical access for laser beams and a fluorescence collection lens. The cell is thermally connected to a ^{3}He refrigerator, giving the cell a base temperature of 450 mK.

Buffer gas enters the cell through a fill line and exits out a 3 mm diameter opening in the side of the cell that faces the discharge source (the ''molecular beam input aperture'' shown in Fig. 1). Helium is continuously supplied to the cell in order to maintain a constant helium atom density in the trapping region.

The constant flow of helium buffer gas out of the cell aperture poses a significant technical problem. The helium gas exiting the aperture can scatter NH radicals out of the incident NH beam. In order to maintain sufficient vacuum in this region just outside the cell, a charcoal coated copper tube (''charcoal tube'') is used to pump away the escaping helium. The charcoal tube is held at 4 K so as to act as a low-profile high-speed vacuum pump. This eliminates any significant scattering of NH radicals.

The helium buffer-gas density in the cell is determined by the rate at which we flow helium into the cell and the conductance out of the molecular beam input aperture. The conductance of the molecular beam input aperture was measured using a fast ion gauge, agreeing with our calculated theoretical value. The absolute buffer-gas density is known to better than 20%.

The NH radicals in the trapping region are detected using laser induced fluorescence (LIF) excited on the $|A\,^3\Pi_2, v' = 0, N' = 1\rangle \leftarrow |X\,^3\Sigma^-, v'' = 0, N'' = 0\rangle$ transition. The excitation laser beam enters the cell and passes through the trap center. Fluorescence from $A \rightarrow X$ is collected by a midplane lens perpendicular to both the laser and molecular beam axes and imaged to the face of a photomultiplier tube (PMT). In this way, time-resolved narrow-band spectra of trapped NH radicals are gathered.

Figure 2 shows a series of time profiles of the number of trapped NH molecules for several different loading times. Shown is the PMT count rate versus time with the LIF excitation frequency set to the peak of the trapped NH spectral feature. As this is a fluorescence experiment, the absolute number of molecules is difficult to determine accurately. By calculating the efficiency of our detection system, excitation probability, and detected molecule fraction we can put a lower bound on our initial number of trapped NH radicals of $>10^8$, which corresponds to a peak density of $>10^8$ cm^{-3}. The data shown in Fig. 2 were taken with ^{4}He with $T = 730$ mK (in order to maintain sufficient ^{4}He density) at a trap depth of 3.3 T. Each trace corresponds to a different duration of loading from the molecular beam source [(a) 10, (b) 100, (c) 200, and (d) 400 ms] and the tail ends of all four traces fit well to a single-exponential decay with time constant of 90 ± 10 ms. The spiky signal during loading is caused by electrical pickup from the dissociation discharge. A buildup to steady-state density during loading can still be seen, as in trace (d). For loading times less than the molecular trap lifetime, the number of trapped molecules increases nearly in proportion with loading time [see curves (a), (b) and (c)]. This demonstrates one of the key features of the continuous

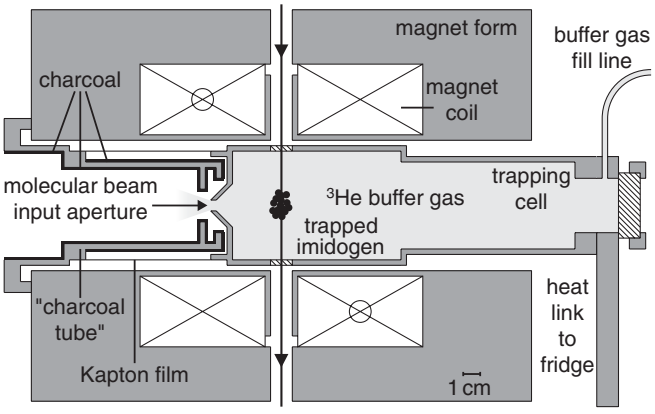

FIG. 1. Schematic diagram of the magnetic trap, buffer-gas cell, and charcoal tube in vacuum. The NH beam is produced by flowing ammonia from a valve through a slit glow discharge 12 cm to the left of the molecular beam input aperture. The radical beam propagates through openings in the 77 and 4 K blackbody radiation shields (not shown), through a section of the magnet bore, through the molecular beam input aperture and into the trapping cell. The trap magnet surrounds the trapping cell and is described in Ref. [41].

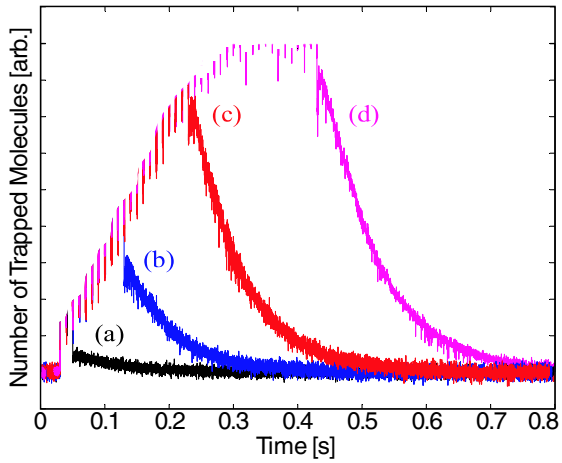

FIG. 2 (color online). Time profiles of the fluorescence signal gathered by the PMT. The curves correspond to different durations of the molecular beam loading of (a) 10, (b) 100, (c) 200, and (d) 400 ms. The dissociation discharge causes periodic over ranging of the signal during loading.

molecular beam loading technique: as the lifetime of molecules in the trap increases, the loading time can be increased resulting in more trapped molecules. Laser ablation sources for buffer-gas loading experiments have to this point shown insignificant increases in numbers trapped from multiple ablation pulses, likely due to the violent nature of the ablation plume in the trapping region. Figure 2(c) and 2(d) shows that as the loading time exceeds the trap lifetime the signal height saturates and there is no longer any significant increase in the number of trapped molecules, as expected. Continuous loading of a room-temperature electrostatic trap has been demonstrated previously [38].

Trapping is spectroscopically verified by tuning the LIF laser to be resonant with high-field-seeking (HFS) molecules and comparing time profiles to low-field seekers (LFS). The HFS molecules quickly leave the trap and are undetectable after 10 ms while the lifetimes of the LFS molecules are enhanced to more than 200 ms at our lowest loading temperature. The spatial sensitivity of our fluorescence collection precludes fitting the spectra for temperature, but we have previously demonstrated rotational and translational thermalization of NH radicals to the buffer-gas temperature [34]. In this experiment, like many atom and molecule trapping experiments, the lifetime of the trapped sample is limited by collisions with the background gas, and the trap lifetimes reported here are comparable to other trapping experiments. Here, *multiple* collisions with background gas atoms are required for a molecule to be lost over the trap edge because the background gas is colder than the trap depth. This allows us to operate at higher background gas pressures than other trapping experiments. Finally, as described below, only trapped molecules produce the lifetimes vs trap depths that we observe.

In the absence of Zeeman relaxation, the trap lifetime will increase significantly as the trap depth increases and the magnetic trapping field holds LFS molecules in the center of the cell. With background buffer gas present, there can be an additional lifetime lengthening factor if collisions with helium atoms enforce diffusive motion and slow the movement of trapped molecules to the walls. Figure 3(a) (inset) shows the measured trap lifetime as a function of $\eta \equiv \mu B_{\max}/k_B T$, where $\mu B_{\max}$ is the trap depth. The lifetime is plotted in units of the field-free diffusion lifetime in the cell, τ_o, given by [39]

$$\tau_o = \frac{16 n \sigma_d}{3\sqrt{2\pi}} \sqrt{\frac{m_{\mathrm{red}}}{k_B T}} \left[\left(\frac{\alpha_1}{R}\right)^2 + \left(\frac{\pi}{h}\right)^2 \right]^{-1}, \qquad (1)$$

where n is the ^{3}He buffer-gas density, σ_d is the thermal average of the diffusion cross section, R and h are the internal radius and length of the cell, m_{red} is the reduced mass of the NH-^{3}He system and α_1 is the first root of the Bessel function J_0 of order zero. For the data in Fig. 3(a) the buffer-gas density was 8.5×10^{14} cm^{-3} and the temperature was 690 mK. The solid curve is a fit of a numerical solution to the diffusion equation including the trap potential [40] and the only fitting parameter is the cross section, yielding a measurement of $\sigma_d = 2.7 \pm 0.8 \times 10^{-14}$ cm^2. The quoted uncertainty is systematic and dominated by uncertainty in the buffer-gas density. Multiplying this by the average relative velocity of NH-^{3}He gives the rate coefficient for energy transport, $k_d = 2.1 \pm 0.6 \times 10^{-10}$ cm^3 s^{-1}. This is in good agreement with the 0.5 K energy transport collision rate of 1.49×10^{-10} cm^3 s^{-1} calculated by Krems *et al.* in Ref. [31].

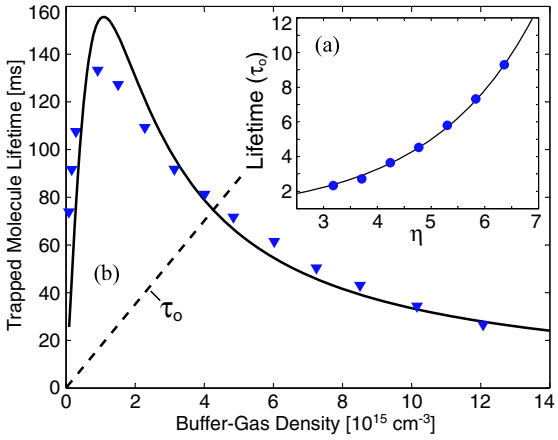

FIG. 3 (color online). Lifetimes for magnetically trapped NH radicals vs (a) trap depth and (b) buffer-gas density. Trapped molecule lifetimes were obtained by fitting the fluorescence to a single-exponential decay. τ_o is the field-free diffusion lifetime calculated from Eq. (1). The solid curve in (b) is a two-parameter fit of the form $1/\tau_{\mathrm{eff}} = A/n + nk_{\mathrm{in}}$ and yields the inelastic cross section.

Figure 3(b) shows the measured trap lifetime for different buffer-gas densities. As the density of the ^{3}He buffer gas is increased from 10^{14} to around 10^{15} cm^{-3} the lifetime of the trapped molecules increases due to the diffusion effect mentioned above. However, as the ^{3}He density is increased past 10^{15} cm^{-3} it is seen that the lifetime decreases. This decrease is due to collision-induced Zeeman relaxation of the NH radicals as they collide with ^{3}He. The time profiles still show good single-exponential decay behavior for these higher buffer-gas densities.

To extract a rate constant for these inelastic collisions, we fit a model curve to the data in Fig. 3. After being loaded, the time profile of the molecule number in the trap can be modeled as $N(t) = N_o e^{-tA/n} e^{-tnk_{\mathrm{in}}}$ where n is the buffer-gas density, N_o is the initial number of NH radicals after loading, and A and k_{in} are fitting parameters corresponding to diffusion enhancement of the lifetime and inelastic collision loss, respectively. This can be rewritten as a single exponential with a time constant given by $1/\tau_{\mathrm{eff}} = A/n + nk_{\mathrm{in}}$, which gives the form for the curve fitted to the data in Fig. 3. The constant k_{in} is the collision-induced Zeeman relaxation rate at 710 mK and is found to be $k_{\mathrm{in}} = 3.0 \pm 0.9 \times 10^{-15}$ cm^3 s^{-1}, corresponding to an inelastic cross section of $\sigma_{\mathrm{in}} = 3.8 \pm 1.1 \times 10^{-19}$ cm^2 and therefore a ratio of diffusive to inelastic cross sections of $\gamma = 7 \times 10^4$. The uncertainties are systematic and are

dominated by uncertainty in the absolute buffer-gas density. This inelastic collision rate is an order of magnitude higher than the 500 mK value of 4.20×10^{-16} cm^3 s^{-1} for 100 Gauss given by Krems *et al.* [31] and may be larger due to the strong temperature dependence of the predicted shape resonance. Furthermore, the rate we measure is averaged over the magnetic field range of our trap, and inelastic collision cross sections are predicted to become strongly field-dependent just below this collision energy [31,32].

In summary, we have demonstrated magnetic trapping of ground state NH molecules using buffer-gas loading from a molecular beam. The energy transport (diffusion) and inelastic collision rate constants for NH-^{3}He have been measured resulting in a ratio of elastic to inelastic collision rates of 7×10^4, which indicates that NH radicals should be amenable to the pumping out of the buffer gas and thermal isolation. It is particularly interesting to note that we are able to trap NH near the shape resonance predicted by Krems *et al.* in Ref. [31]. Trapping at lower temperatures may increase the number trapped and perhaps allow for sympathetic cooling of large numbers of molecules.

We thank Katsunari Enomoto and Michael Gottselig for their valuable assistance in the design and fabrication of the apparatus and also greatly acknowledge Colin Connolly for his construction of the ^{3}He refrigerator used in these experiments. The authors are grateful to B. Friedrich and R. Krems for discussions and careful reading of the manuscript and G. C. Groenenboom for helpful discussions. This work was supported by the U.S. Department of Energy under Contract No. DE-FG02-02ER15316 and the U.S. Army Research Office.

*Electronic address: wes@cua.harvard.edu
†Present address: Max-Planck-Institut für Quantenoptik, Garching, Germany.

[1] J. Doyle, B. Friedrich, R. V. Krems, and F. Masnou-Seeuws, Eur. Phys. J. D **31**, 149 (2004).
[2] H. L. Bethlem and G. Meijer, Int. Rev. Phys. Chem. **22**, 73 (2003).
[3] D. DeMille, Phys. Rev. Lett. **88**, 067901 (2002).
[4] A. André, D. DeMille, J. M. Doyle, M. D. Lukin, S. E. Maxwell, P. Rabl, R. J. Schoelkopf, and P. Zoller, Nature Phys. **2**, 636 (2006).
[5] A. Micheli, G. K. Brennen, and P. Zoller, Nature Phys. **2**, 341 (2006).
[6] M. G. Kozlov and L. N. Labzowsky, J. Phys. B **28**, 1933 (1995).
[7] S. Schiller and V. Korobov, Phys. Rev. A **71**, 032505 (2005).
[8] N. Balakrishnan and A. Dalgarno, Chem. Phys. Lett. **341**, 652 (2001).
[9] R. V. Krems, Int. Rev. Phys. Chem. **24**, 99 (2005).
[10] J. L. Bohn, A. V. Avdeenkov, and M. P. Deskevich, Phys. Rev. Lett. **89**, 203202 (2002).
[11] A. V. Avdeenkov, M. Kajita, and J. L. Bohn, Phys. Rev. A **73**, 022707 (2006).
[12] G. S. F. Dhont, J. H. van Lenthe, G. C. Groenenboom, and A. van der Avoird, J. Chem. Phys. **123**, 184302 (2005).
[13] M. Kajita, Phys. Rev. A **74**, 032710 (2006).
[14] M. Lara, J. L. Bohn, D. Potter, P. Soldan, and J. M. Hutson, Phys. Rev. Lett. **97**, 183201 (2006).
[15] J. M. Sage, S. Sainis, T. Bergeman, and D. DeMille, Phys. Rev. Lett. **94**, 203001 (2005).
[16] E. A. Donley, N. R. Claussen, S. T. Thompson, and C. E. Wieman, Nature (London) **417**, 529 (2002).
[17] H. L. Bethlem, G. Berden, and G. Meijer, Phys. Rev. Lett. **83**, 1558 (1999).
[18] R. Fulton, A. I. Bishop, M. N. Schneider, and P. F. Barker, J. Phys. B **39**, S1097 (2006).
[19] M. S. Elio, J. J. Valentini, and D. W. Chandler, Science **302**, 1940 (2003).
[20] J. D. Weinstein, R. deCarvalho, T. Guillet, B. Friedrich, and J. M. Doyle, Nature (London) **395**, 148 (1998).
[21] J. M. Bakker, M. Stoll, D. R. Weise, O. Vogelsang, G. Meijer, and A. Peters, J. Phys. B **39**, S1111 (2006).
[22] R. deCarvalho, N. Brahms, B. Newman, J. M. Doyle, D. Kleppner, and T. Greytak, Can. J. Phys. **83**, 293 (2005).
[23] D. M. Silveira, O. Pereira, M. Veloso, and C. L. Cesar, Braz. J. Phys. **31**, 203 (2001).
[24] J. D. Weinstein, R. deCarvalho, K. Amar, A. Boca, B. C. Odom, B. Friedrich, and J. M. Doyle, J. Chem. Phys. **109**, 2656 (1998).
[25] K. Maussang, D. Egorov, J. S. Helton, S. V. Nguyen, and J. M. Doyle, Phys. Rev. Lett. **94**, 123002 (2005).
[26] M. Stoll (private communication).
[27] N. L. Garland and D. R. Crosley, J. Chem. Phys. **90**, 3566 (1989).
[28] G. A. Raiche, J. B. Jeries, K. Rensberger, and D. R. Crosley, J. Chem. Phys. **92**, 7258 (1990).
[29] C. D. Ball and F. C. D. Lucia, Phys. Rev. Lett. **81**, 305 (1998).
[30] R. V. Krems and A. Dalgarno, J. Chem. Phys. **120**, 2296 (2004).
[31] R. V. Krems, H. R. Sadeghpour, A. Dalgarno, D. Zgid, J. Kłos, and G. Chałasiński, Phys. Rev. A **68**, 051401 (2003).
[32] H. Cybulski, R. V. Krems, H. R. Sadeghpour, A. Dalgarno, J. Kłos, G. C. Groenenboom, A. van der Avoird, D. Zgid, and G. Chałasinski, J. Chem. Phys. **122**, 094307 (2005).
[33] S. Y. T. van de Meerakker, I. Labazan, S. Hoekstra, J. Küpper, and G. Meijer, J. Phys. B **39**, S1077 (2006).
[34] D. Egorov, W. C. Campbell, B. Friedrich, S. E. Maxwell, E. Tsikata, L. D. van Buuren, and J. M. Doyle, Eur. Phys. J. D **31**, 307 (2004).
[35] H. Lewandowski, L. P. Parazzoli, D. Lobser, and C. Romero, in 379.WE-Heraeus-Seminar on Cold Molecules (2006).
[36] S. Y. T. van de Meerakker, B. G. Sartakov, A. P. Mosk, R. T. Jongma, and G. Meijer, Phys. Rev. A **68**, 032508 (2003).
[37] Alloy C10100, annealed in forming gas.
[38] T. Rieger, T. Junglen, S. A. Rangwala, P. W. H. Pinske, and G. Rempe, Phys. Rev. Lett. **95**, 173002 (2005).
[39] J. B. Hasted, *Physics of Atomic Collisions* (American Elsevier, New York, 1972), 2nd ed., Chap. 1.6.
[40] J. D. Weinstein, Ph.D. thesis, Harvard University 2001.
[41] J. G. E. Harris, R. A. Michniak, S. V. Nguyen, W. C. Campbell, D. Egorov, S. E. Maxwell, L. D. van Buuren, and J. M. Doyle, Rev. Sci. Instrum. **75**, 17 (2004).